Eksploatacja i Niezawodnosc - Maintenance and Reliability
Volume 29 (2027), Issue 3
https://ein.org.pl
The Polish Maintenance Society

Effect of tool wear on the surface layer properties and fatigue life of milled Ti6Al4V titanium alloy components

Jakub Matuszak[1,*], Kazimierz Zaleski[1], Andrzej Zyśko[2]

[1] Lublin University of Technology, Poland
[2] The Institute of Technical Sciences and Aviation, Państwowa Wyższa Szkoła Zawodowa w Chełmie, Poland
* Corresponding Author: j.matuszak@pollub.pl

Received: 6 May 2026
Revised: 2 October 2026
Accepted: 30 October 2026
Online: 16 November 2026

This is an open access article under the CC BY 4.0 license

Abstract

Ti6Al4V titanium alloy is widely used in the aerospace, biomedical, and chemical industries due to its excellent mechanical properties and corrosion resistance. This study investigates the effect of milling cutter flank wear (VB_3 = 0–0.45 mm) on the surface layer properties and fatigue life of Ti6Al4V titanium alloy specimens. Progressive tool wear caused a slight increase in surface roughness (Sa increased from 0.75 µm to 0.90 µm). Compressive residual stresses increased from −152 MPa to −245 MPa, with their depth rising from 40 µm to 128 µm. The degree of work hardening increased from 5.5% to 8.6%, and the hardening depth rose from 20 µm to 29 µm. The results reveal a competition between the detrimental effect of increased surface roughness and the beneficial effect of compressive residual stresses on fatigue performance, with the latter proving dominant: despite increased roughness, fatigue life improved by approximately 16%. The results demonstrate that milling conducted with the conditions applied in the study can be recommended as a finishing operation for Ti6Al4V components.

Keywords: *Ti6Al4V titanium alloy, milling,, surface roughness, thrust force, residual stresses, fatigue life*

Article citation:
Matuszak J, Zaleski K, Zyśko A, Effect of tool wear on the surface layer properties and fatigue life of milled Ti6Al4V titanium alloy components, Eksploatacja i Niezawodnosc – Maintenance and Reliability 2027: 29(3) http://doi.org/10.17531/ein/242345

Highlights

- Flank wear of a milling cutter affects the surface layer properties of Ti6Al4V alloy.
- Progressive tool wear increases the surface roughness parameter Sa from 0.75 to 0.90 µm, remaining within acceptable limits for finishing operations.
- Compressive residual stresses increase from −152 MPa to −245 MPa, with their depth rising from 40 µm to 128 µm, enhancing fatigue resistance.
- Work hardening degree and hardening depth increase with progressive tool wear.
- Tool wear causes ~16% improvement in fatigue life due to compressive residual stresses.

1. Introduction

In machining processes, cutting tools operate under severe conditions due to high temperature generated in the cutting zone [1,2] heavy mechanical loads [3,4], and friction on the rake and flank tool's faces [5,6]. When exposed to such conditions, cutting edges undergo relatively rapid wear [7]. This wear may progress, which is characterized by a gradual increase in tool wear indicators such as the flank wear land width [8]. Another wear mode is discontinuous wear, also referred to as catastrophic wear, which is manifested as a sudden loss of cutting performance, for example, due to tool edge breakage [9].

The wear of cutting tool edges depends on numerous factors, among which the workpiece material and its microstructure play a major role [10,11]. Titanium and its alloys are classified as difficult-to-machine materials, with the associated difficulties manifested, among others, by a rapid increase in cutting edge wear [12]. The poor machinability of titanium alloys is attributed to their specific properties such as low thermal conductivity, low Young's modulus, and a tendency to form built-up edge and frictional adhesions during cutting [13,14]. The high compressive load on the tool's working surfaces combined with the low thermal conductivity of the workpiece material leads to a significant increase in the cutting tool temperature [15], which adversely affects tool life. The chemical composition and microstructure of the machined

titanium alloy also have a significant influence on tool wear. Machining titanium alloys with better machinability in terms of tool wear allows the use of higher cutting speeds at a specified tool life. As demonstrated by P.-J. Arrazola et al., the machining of Ti-6Al-4V at a cutting speed of 80 m/min for 15 min resulted in the same tool wear as that obtained in the machining of the Ti-555.3 alloy under identical time conditions at a cutting speed of 45 m/min [16].

Tool wear largely depends on the cutting tool's material. A study by H. Su showed that the use of polycrystalline diamond (PCD) tools for milling titanium alloy TA15 enabled a substantial increase in cutting speed while maintaining high tool life [17]. Research on the influence of carbide grain size in end mills on the tool life in milling Ti-6Al-4V titanium alloy showed that tools with an ultrafine-grained structure exhibited the lowest wear rate and the highest resistance to catastrophic failure [18]. Titanium alloys are also machined using tools coated with wear-resistant protective layers. The results a study on the influence of wear-resistant coatings applied on cemented carbide inserts on the tool wear in the milling of Ti-6242S titanium alloy are reported in [19].

Another group of factors influencing cutting tool wear includes cutting parameters and cooling method. Bandapallia C. et al. investigated the effect of cutting speed in the micro-milling of Ti-0.3Mo-0.8Ni titanium alloy on tool wear [3]. E. Liu et al. investigated the wear of cemented carbide tools during the cryogenic machining of T-5553 titanium alloy in liquid nitrogen [20]. The beneficial effect of hybrid lubrication and cooling on the tool life in machining Ti-3Al-2.5V titanium alloy was demonstrated in [21]. A study by R. Gaddam et al. showed that cooling efficiency and tool life in the milling of Ti-6Al-4V titanium alloy could be improved by increasing the coolant flow through the appropriate tool geometry design [22]. R.B. Da Silva et al. demonstrated that tool life in the high-speed machining of Ti-6Al-4V was also affected by the pressure of the supplied coolant [23]. A reduction in milling tool wear as a result of increased coolant pressure in titanium alloy machining was reported in [24].

Numerous researchers have addressed the mechanism of tool wear in the machining of titanium alloys. M. Li observed that diffusion had a significant influence on the wear of cemented carbide inserts used for milling Ti-6Al-4V [25]. An analysis of the physical wear mechanisms of uncoated and multilayer coated inserts used for finish milling of titanium alloys showed the occurrence of adhesive, diffusion and, in the case of coated inserts, delamination wear [26]. A neural-network-based model enabling the prediction of tool wear in the milling process of a titanium alloy was developed in [27]. A finite element method (FEM) simulation model of tool wear during the cutting of Ti6Al4V titanium alloy exhibited a strong correlation with experimental data [28]. Findings on the wear mechanism of PCD cutting edges in titanium alloy machining were reported in [29]. The wear mechanism of diamond tools during ultra-precision cutting of pure titanium and Ti6Al4V titanium alloy was studied in [30]. Y. Wang et al. [31] examined the wear behavior of cermet micro-mills during the machining of microchannels in titanium alloys. Comparative research on the wear mechanisms of ceramic and cemented carbide tools during the machining of Ti6Al4V titanium alloy was carried out by Tan et al. [32]. The tool wear mechanism during the milling of Ti-5Al-5Mo-5V-1Cr-1Fe titanium alloy is described in [33].

Various machining methods are utilized in the manufacturing of titanium alloy components. Given the complex geometry of many titanium alloy parts, especially those used in the aerospace industry, milling is a crucial manufacturing method [34,35]. Milling should provide the specified dimensional and shape accuracy as well as the desired surface integrity. For the adhesive joining of milled elements, it is critical to ensure proper adhesive properties [36]. Many studies have been dedicated to investigating the surface roughness of titanium alloys after milling. Research by I. Daniyan et al. showed that the surface roughness of milled Ti6Al4V titanium alloy components depended on the cutting tool design [37]. The surface roughness of titanium alloys was also affected by the milling parameters. Study [38] examined the impact of cutting speed on the surface roughness of titanium alloy Ti6Al4V produced by additive manufacturing. Kishore Kumar et al. observed that cutting speed and feed rate had the greatest impact on the surface roughness of Grade-5 and Grade-12 titanium alloys after micro-milling with cemented carbide tools [39]. According to X. Wu et al., the surface roughness of the additively-manufactured Ti6Al4V alloy after micro-milling was most significantly influenced by feed per tooth, tool nose radius, and bottom edge inclination angle [40]. In [41], the

authors studied the influence of ultrasonic-assisted milling of titanium alloy and polymer composite on the resulting surface roughness. M.H. Ali found, through experimental testing and FEM modeling of Ti6Al4V face milling, that surface roughness was directly proportional to feed cutting force [42]. The authors of [43] optimized the milling parameters for the Ti6Al4V alloy using a ball-end mill, considering the surface roughness parameter Rq and machining time. The impact of cutting speed, feed, and cutting tool helix angle on surface roughness in the peripheral milling of the Ti6Al4V alloy was studied by G. Sur et al. [44].

Surface texture and machining accuracy depend on the wall thickness of milled components. A. Polishetty et al. [45] investigated the effect of trochoidal milling parameters on the Ra surface roughness and thickness errors of thin-walled Ti6Al4V titanium alloy elements. The results of a study determining the influence of milling strategies for thin-walled Ti6Al4V titanium alloy components on their surface roughness and geometric accuracy were presented in [46]. The authors of [47] developed a dynamic model for milling thin-walled titanium alloy elements, accounting for the stiffness of both the tool and the workpiece, which allowed for the determination of vibration stability during machining. Experimental research and FEM analysis showed that errors related to the deformation of thin-walled Ti6Al4V alloy components during milling could be reduced by employing an improved workpiece clamping method [48]. The dimensional and geometric accuracy of thin-walled titanium alloy specimens that were milled with a horizontal orientation on the machine tool was studied by S. Kurpiel et al. [49].

The operational durability of manufactured components largely depends on the physical properties of their surface layer, such as microstructure, microhardness, and residual stresses. The combination of these geometrical, physical-mechanical, and stress-strain characteristics of the surface layer is collectively referred to as surface integrity, a concept that has been widely adopted to describe and assess the functional quality of machined components. In this context, machining parameters should be considered not only as means of shaping but also as tools for the purposeful formation of the operational properties of manufactured component [50]. To improve these properties, shot peening is often introduced as an additional operation [51]. Furthermore, the technological milling conditions also influence the physical properties of the surface layer of machined titanium alloy workpieces. According to C. Chen et al. [52], the application of interpass milling for additively-manufactured TC4 titanium alloy has a beneficial effect on the surface layer microstructure, microhardness, and tensile strength of the machined specimens. An experimental study by A. Shokrani et al. [53] showed that the application of cryogenic cooling with liquid nitrogen during the end milling of Ti6Al4V titanium alloy improved the surface layer properties and reduced microscopic surface defects. The use of a hybrid CO_2 + MQL cooling and lubrication strategy in Ti6Al4V alloy milling led to a substantial enhancement of surface microhardness relative to conventional flood cooling [54]. Tool orientation in the ball-end milling of the TC17 alloy had a more significant impact on residual stresses than surface microhardness, according to [55]. The impact of cutting speed and tool wear on the microstructure and microhardness profile of the surface layer in Ti-1023 titanium alloy milling was studied by Y. Houchuan et al. [56]. M. Wimmer et al. demonstrated that residual stresses in the surface layer of Ti6Al4V after peripheral milling were governed by the cutting conditions and the cutting edge rounding [57]. Study [58] compared the residual stress distributions in the surface layer of a titanium alloy after milling, measured by the layer removal method and X-ray diffraction. A. Robles et al. presented a model for predicting residual stresses generated during the face milling of Ti6Al4V titanium alloy, which was validated with experimental data obtained by the X-ray diffraction method [59].

Fatigue life is a key operational attribute determined by surface layer properties. T. Childerhouse et al. [60] studied the impact of milling the Ti6Al4V alloy with polycrystalline diamond and coated carbide tools on the fatigue performance of machined parts. According to D. Yang et al., the fatigue life of milled Ti6Al4V alloy samples depended on the cutting parameters, with feed rate having the greatest impact, followed by cutting speed and depth of cut [61]. The influence of cutting speed on the tool wear, surface layer properties, and fatigue life of Ti6Al4V titanium alloy samples face-milled with a cemented carbide cutter was presented in [62].

Numerous publications on the machining of titanium alloys

confirm the great importance of this alloy as a valuable structural material. The specific properties of titanium alloys give rise to intensive wear of cutting tools during machining. A significant aspect of titanium alloy machining concerns the impact of tool wear on the surface layer condition and functional properties of machined workpieces. While the individual effects of tool wear on surface roughness, residual stresses, and microhardness have been reported in the literature, a comprehensive experimental study simultaneously correlating progressive flank wear with all these surface layer parameters and, critically, with the resulting fatigue life of milled Ti6Al4V components is lacking. In particular, the competition between the detrimental effect of increased surface roughness and the beneficial effect of compressive residual stresses on fatigue performance, as a function of tool wear progression, has not been systematically addressed. The present study fills this gap by providing an integrated experimental dataset obtained under controlled milling conditions. The aim of this study is to evaluate the influence of cutter blade wear on the surface roughness, residual stresses, surface layer microhardness, and fatigue life of milled Ti6Al4V titanium alloy parts.

2. Materials and methods

Experiments were carried out on specimens made of the Ti6Al4V titanium alloy. The selection of this alloy was determined by its widespread application in the manufacture of structural components in the aerospace, shipbuilding, and chemical industries, as well as in the production of surgical implants. The chemical composition of the Ti6Al4V alloy was as follows: aluminum – (6.25–6.31)%, vanadium – (4.09–4.12)%, iron – (0.18–0.21)%, carbon – (0.026–0.027)%, titanium – balance. This alloy is characterized by very good corrosion resistance, no harmful effects on the human body, and high strength (Rm = 1014 MPa). The Young's modulus of this alloy is 120 GPa and its hardness is 33 HRC.

Three types of Ti6Al4V titanium alloy specimens were used in the study:

- S1 specimens – in the shape of a rectangular prism with the dimensions of 150 × 90 × 40 mm – intended for milling cutter wear tests and cutting force measurements,
- S2 specimens – in the shape of a rectangular prism with the dimensions of 100 × 15 × 4.5 mm – intended for surface topography and roughness measurements, residual stress distribution analysis, and microhardness testing of the surface layer,
- S3 specimens – in the shape shown in Fig. 1 – intended for fatigue life testing.

Following their machining to the required shape and dimensions, the specimens were subjected to stress-relief annealing in a vacuum furnace, which enabled the removal of residual stresses generated during the manufacturing process.



(a)



(b)

Figure 1. Titanium alloy specimen used for fatigue life testing: (a) actual view, (b) 3D model with the specimen's dimensions.

The prepared samples were used to study the effect of milling cutter blade wear on the surface texture parameters of the machined surface, the distribution of residual stresses, the microhardness of the surface layer, and the fatigue life of the Ti6Al4V titanium alloy after milling. The adopted research plan is schematically presented in Fig. 2.

Samples S1, S2, and S3 were subjected to milling, which was carried out on a vertical machining center Avia VMC800HS equipped with a Heidenhain iTNC530 control system. Two-flute indexable milling cutters Seco Tools R217.21-1820.0-LP06.2A with a diameter of 20 mm and internal coolant supply were used as cutting tools. Two rectangular cutting inserts LPHT060310ER-E05 made of cemented carbide grade MM4500, manufactured by Seco Tools, were mounted in the tool body. To investigate the effect of cutter edge wear on surface layer properties and fatigue life, samples S1 were milled to achieve a specified degree of wear of the cutting insert edges. The VB_3 wear index (according to ISO 8688-2) was adopted as the measure of cutting edge wear. In the study, both "new" inserts ($VB_3 = 0$) and inserts with different degrees of wear were

used, with VB_3 values of 0.15 mm, 0.30 mm, and 0.45 mm, respectively (the permissible deviation of the VB_3 was set at+0.05 mm). According to ISO 8688-2, the end-of-life criterion for milling tools is defined as VB_3 = 0.3 mm averaged over all cutting edges, or VB_3= 0.5 mm on any single edge. In the present study, the investigated wear range (VB_3 = 0 - 0.45 mm) intentionally extends beyond the standard tool-life criterion in order to evaluate the effect of progressive flank wear on surface layer properties and fatigue performance. The results demonstrate that even at VB_3 = 0.45 mm, the obtained surface roughness and fatigue life remain acceptable for a finishing operation on Ti6Al4V components. Measurements of the cutter edge wear index were carried out using a Keyence VHX-500 microscope. Samples intended for surface layer and fatigue life investigations were machined using cutters with their edge wear values of VB_3 = 0, 0.15 mm, 0.30 mm, and 0.45 mm. The cutting parameters were maintained constant as follows:

- depth of cut a_p = 0.5 mm,
- milling width a_e = 7.5 mm,
- feed per tooth f_z = 0.2 mm/tooth,
- cutting speed v_c = 70 m/min.



Figure 2. Scheme of the research plan.

The cutting parameters were selected based on the tool manufacturer's recommendations for machining Ti6Al4V with cemented carbide indexable inserts, as well as on preliminary trials aimed at ensuring stable cutting conditions and representative surface layer formation. A Mobil Cut fluid was used during the milling process.

The 4.5 mm thick S2 samples had only one surface milled to, remove a 0.5 mm thick layer of material, whereas the 5 mm thick S3 samples had two opposite surfaces milled, resulting in a total thickness reduction of 1 mm. Following the milling process, both S2 and S3 samples reached a final thickness of 4 mm.

The surface texture parameters of the samples milled with tools of varying tool wear were examined using a Hommel Etamic T8000RC 120-140 profilometer. The topography was determined for a surface area of 4.8 mm x 4.8 mm using a TKU 300/600 measuring head at a Vt feed speed of 0.5 mm/s. The measurements were repeated 5 times for each wear level, and a statistical significance analysis of the effect of the wear indicator VB_3 on the Sa and Sz surface texture parameters was performed. The following surface texture parameters were measured:

- Sa – arithmetical mean height of the surface,
- Sz – maximum height of the surface,
- Sp – maximum peak height,
- Sv – maximum pit depth.

Thrust force measurements were carried out using a Kistler 9125A dynamometer equipped with a Kistler type 5070 amplifier. The measured signals were recorded using Dynoware software (type 2825A) with a Dynoware data acquisition card (type 5697A). From the stable force signal (excluding the entry and exit zones), the mean values and thrust force amplitudes were determined. Each experiment was repeated 8 times; the cutting inserts were replaced every 2 trials to maintain the assumed wear level within the specified tolerance and prevent progression to the next wear stage.

The microhardness testing of the surface layer was carried out on samples with oblique cross-sections, using an LM700AT microhardness tester manufactured by Leco. The Vickers method was applied, using an indenter with a load of 50 g.

The residual stress distribution in the surface layer of the S2 samples that were machined using cutters with varying degrees of tool wear was investigated via a mechanical method. The values of residual stresses were calculated based on the deformation of the tested samples resulting from a successive removal of material layers wherein the residual stresses were present. The material layers were removed by chemical etching

using a 4% aqueous solution of hydrofluoric acid. The measurements were repeated 5 times for each VB_3 wear level.

Fatigue life tests were conducted on the S3 specimens with a reduced width in the central section. Individual specimens were machined on both sides using a cutter with the same degree of tool wear, while maintaining identical cutting conditions. The fatigue tests were carried out on a dedicated test stand, the operating principle of which is schematically shown in Fig. 3. The measurements were repeated 5 times for each VB_3 wear level.

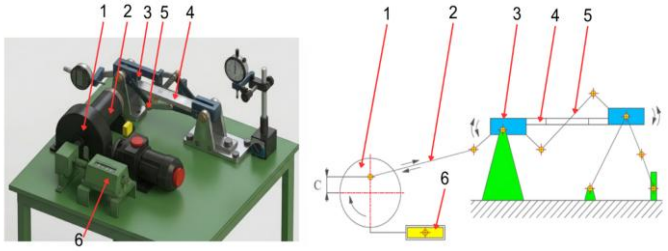

Figure 3. Schematic diagram of a fatigue life test stand.

A drive from motor 1 is transmitted via the eccentric mechanism 2 and a connecting rod 3 to a lever system 5, which induces symmetrical, alternating bending of a specimen 4. The tests were conducted at a fixed bending amplitude of the specimen. Fatigue life was quantified by the number of bending cycles (counter reading 6) until specimen fracture. The value of the bending amplitude at which fracture occurred after exceeding 10^5 bending cycles was determined by adjusting the radius on an eccentric 2.

3. Results and discussion

The study into the effect of the wear of the cutting edges of cemented carbide inserts, mounted in the bodies of indexable milling cutters, on the surface layer properties and fatigue life of milled Ti6Al4V titanium alloy specimens was preceded by 'wearing' these inserts to obtain three different values of the flank wear indicator VB_3 (0.15 mm, 0.3 mm, and 0.45 mm). The cutting inserts with the desired degree of wear were fabricated by milling the S1 specimens of Ti6Al4V titanium alloy using tools equipped with these inserts on an Avia VMC800HS vertical machining center. Images of the flank surface of a sharp (new) and a 'worn' insert (VB_3 = 0.45 mm) is shown in Fig. 4. Based on the microscopic observations, the dominant wear mechanism on the flank face is abrasive wear, accompanied by adhesion of the workpiece material within the cutting edge zone, mechanisms characteristic of cemented carbide tools during the machining of titanium alloys, as reported in [25,26].

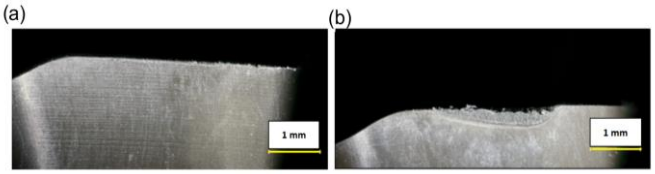

Figure 4. Sharp (new) cutting insert (a) and worn insert (b).

The wear of the cutting tool edges changes their geometry. The surface topography of the workpiece formed by the cutting process largely depends on the kinematic–stereometric mapping of the tool edge in this workpiece material. Therefore, the wear-induced change in the shape of the cutting edge affects the surface texture of the machined surface: the increasing flank wear land alters the effective cutting geometry, raises cutting forces, and promotes vibrations during milling, all of which contribute to the observed deterioration of surface texture regularity. Fig. 5 shows the surface topography of a Ti6Al4V alloy specimen that was machined with a sharp tool (a) and with a tool whose flank wear indicator VB_3 was 0.45 mm.

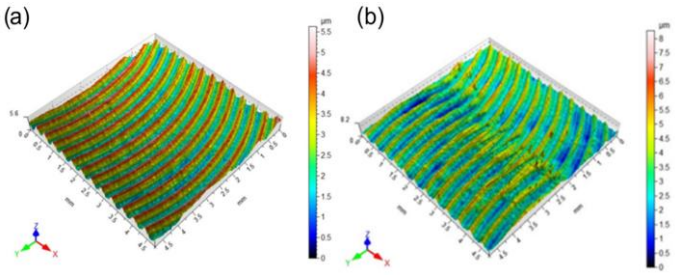

Figure 5. Surface topography after milling: (a) with a sharp tool (VB_3 = 0), (b) with a tool with a specified degree of wear (VB_3 = 0.45 mm).

The surface of a specimen that was milled with a sharp cutter is characterized by the presence of regular peaks of micro-roughness in the form of arcs corresponding to the cutter radius, located at approximately equal distances related to the feed per tooth (Fig. 5a). In contrast, the surface of a specimen that was milled with a worn tool exhibits disturbances in the surface texture. Random, irregular depressions and intersecting machining marks are visible, which can be associated with the re-cutting (idle) passage of the tool edge (Fig. 5b).

Fig. 6 shows the influence of cutter flank wear on the Sa and Sz parameters of surface topography. The value of the Sz parameter is approximately (7–9) times higher than that of Sa, indicating the presence of isolated peak and valley extremes that

significantly exceed the mean surface amplitude. This ratio suggests that the machined surface, while relatively uniform in its average texture, contains localized irregularities that may act as stress concentrators under cyclic loading. As the tool wear increases, which is expressed by the VB_3 indicator, a slight increase in the surface roughness is observed, this increase being more pronounced for the Sz parameter. After milling with tool described by VB_3 = 0.45 mm, the Sz parameter increases by approximately 55% compared to the surface machined with a sharp tool, whereas for the Sa parameter this increase is about 20%.

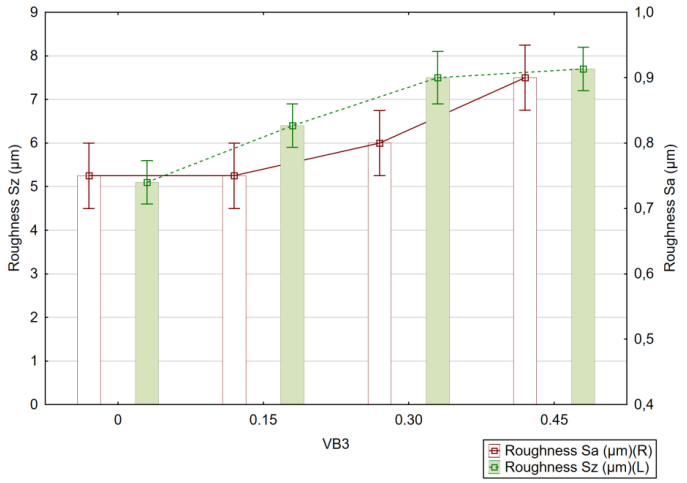

Figure 6. Effect of tool wear on the surface roughness parameters Sa and Sz.

To assess the statistical significance of the effect of the wear indicator VB_3 on the surface texture parameters Sa and Sz, a one-way analysis of variance (ANOVA) was performed at a significance level of $\alpha = 0.05$. The normality of the investigated variables was confirmed by the Shapiro-Wilk test, and the homogeneity of variances was verified by Levene's test, which validated the application of ANOVA (Table 1).

Table 1. Results of the ANOVA analysis of the effect of the wear indicator VB_3 on the surface texture parameters Sa and Sz, where df – number of degrees of freedom, SS – sum of squares between groups, MS – mean sum of squares between groups, F – value of the test statistic, p – probability level.

Sa						
Variable	SS	df	MS	F	p	Partial Eta Squared
VB_3	0.07306	3	0.02435	10.576	0.000446	0.664750
Sz						
VB_3	21.4379	3	7.1460	25.751	0.000002	0.828426

The results of the ANOVA analysis (Table 1) indicate that the flank wear indicator VB_3 has a statistically significant effect on both Sa and Sz, with statistically significant differences in the mean values of Sa and Sz observed across the investigated wear levels. The obtained partial eta-squared values indicate that the surface roughness parameter Sz is more strongly dependent on the wear indicator VB_3 than Sa.

The ANOVA results indicate that statistically significant differences in the mean values of the surface texture parameters Sa and Sz exist between the groups corresponding to the investigated wear levels. To determine which specific groups differ significantly from one another, a post-hoc test (Tukey's test) was applied.

Table 2 presents the results of Tukey's test for the dependent variables Sa and Sz. The analysis shows that a change in wear level from VB_3 = 0 mm to VB_3 = 0.15 mm, from VB_3 = 0 mm to VB_3 = 0.30 mm, and from VB_3 = 0.15 mm to VB_3 = 0.30 mm does not have a statistically significant effect on the surface texture parameter Sa. In the case of Sz, the lack of statistically significant differences occurs only when the wear indicator changes from VB_3 = 0.30 mm to VB_3 = 0.45 mm.

Table 2. Comparative analysis of the significance of differences (post-hoc Tukey's test) between the mean values of the surface roughness parameters Sa and Sz after milling with tools of varying wear levels (indicator VB_3).

Sa				
VB_3	0	0.15	0.30	0.45
0.0		**0.999208**	**0.381863**	0.000907
0.15	**0.999208**		**0.451724**	0.001131
0.30	**0.381863**	**0.451724**		0.021445
0.45	0.000907	0.001131	0.021445	
Sz				
VB_3	0	0.15	0.30	0.45
0.0		0.006366	0.000191	0.000187
0.15	0.006366		0.021155	0.006366
0.30	0.000191	0.021155		**0.930553**
0.45	0.000187	0.006366	**0.930553**	

Fig. 7 shows the effect of the tool flank wear indicator VB_3 on the height of surface roughness peaks and the depth of surface roughness valleys after milling. An increase in the tool wear leads to an increase in both the maximum height of surface roughness peaks (Sp) and the maximum depth of surface roughness valleys (Sv). The surfaces that were machined using both sharp (unworn) tools and tools with varying degrees of wear exhibit a slightly higher (by approximately 3–11%) value of the Sv parameter compared to the Sp parameter.

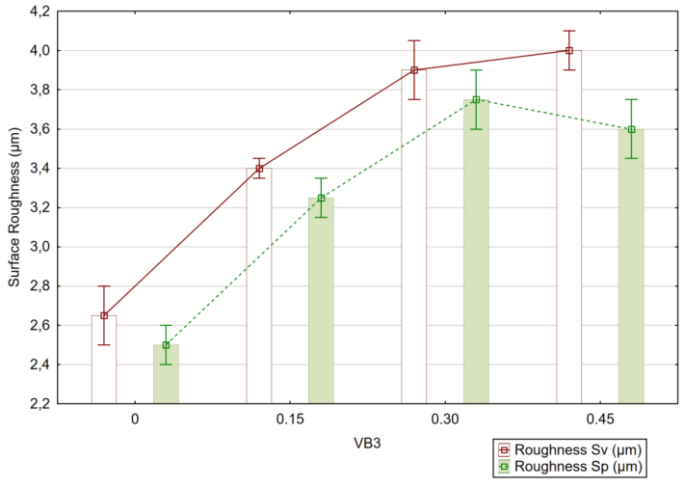

Figure 7. Effect of tool edge wear on the surface roughness parameters Sp and Sv.

The observed increase in the surface roughness parameters with tool wear progression is likely associated with the changes in tool edge geometry caused by wear, and consequently with changes in the shape of machining marks left in the workpiece material by the moving cutting edges. The wear of the flank face leads to an increase in the friction area between the cutting edge and the workpiece material, which may result in an increase in the cutting forces. Due to the high friction coefficient and low Young's modulus of the tested titanium alloy, one must consider the generation of tool and workpiece vibrations during milling, as this phenomenon has an adverse effect on surface roughness.

Figure 8 shows an example of the thrust force course during milling. The entry zone, the stable machining zone, and the moment of tool exit from the cutting zone are clearly visible.

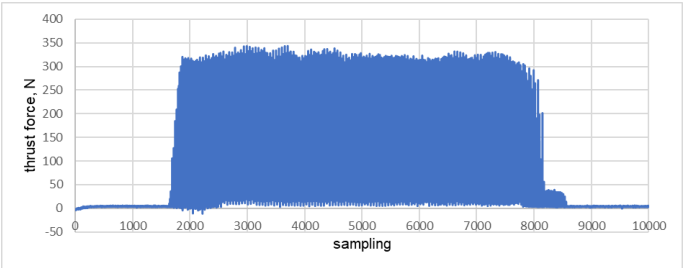

Figure 8. Thrust force course during milling ($VB_3 = 0$).

Figure 9 shows the effect of milling cutter flank wear on the thrust force and thrust force amplitude. With increasing VB_3, the mean thrust force increases progressively from approximately 250 N for a sharp tool to 670 N at $VB_3 = 0.45$ mm, representing a approximately 2.7-fold increase. A similar trend is observed for the thrust force amplitude, which rises from approximately 230 N to 610 N over the same wear range. The substantial increase in both quantities with progressive tool wear confirms the enlargement of the contact area between the worn flank face and the workpiece, resulting in higher mechanical loads acting on the machined surface — a factor directly contributing to the observed increase in compressive residual stresses and surface layer hardening.

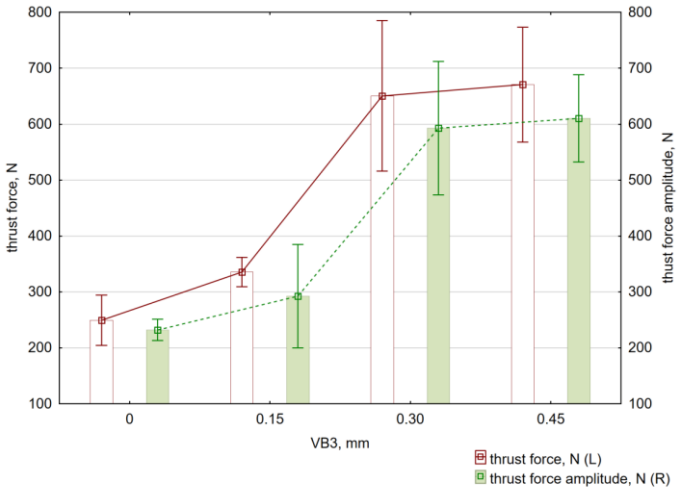

Figure 9. Effect of milling cutter flank wear VB_3 on thrust force and thrust force amplitude.

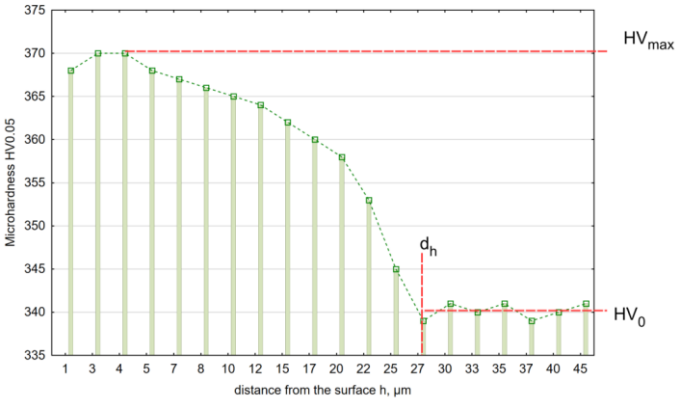

Figure 10. Microhardness distribution in the specimen machined using a milling cutter with $VB_3 = 0.45$ mm.

In the cutting process, the cutting edge acting on the workpiece material causes plastic deformations to occur both in the region of the cut layer and at a certain depth beneath the machined surface. This deformation results in increased hardness of the surface layer formed during machining. The observed changes in material hardness caused by machining occur within a layer of very small thickness. Therefore, these changes are evaluated based on microhardness measurements. An example of a microhardness distribution in the surface layer of a Ti6Al4V alloy specimen milled using a tool with $VB_3 =$

0.45 mm is presented in Fig. 10.

Based on the surface layer microhardness distribution curves for the specimens machined using milling cutters with varying degrees of tool wear, the following quantities were determined:

HV_{max} – maximum microhardness of the surface layer,

HV_0 – microhardness of the specimen core,

d_h – hardening depth.

Based on the above quantities, the degree of work hardening of the surface layer was determined according to the following relationship:

$$e = 100\frac{HV_{max}-HV_0}{HV_0}, \%, \quad (1)$$

The maximum microhardness occurs at a small depth beneath the machined surface, and an increase in this depth causes the microhardness to decrease to a value corresponding to the core microhardness of the material. The effect of milling cutter tool wear on the degree of work hardening of the surface layer and hardening depth is presented in Fig. 11.

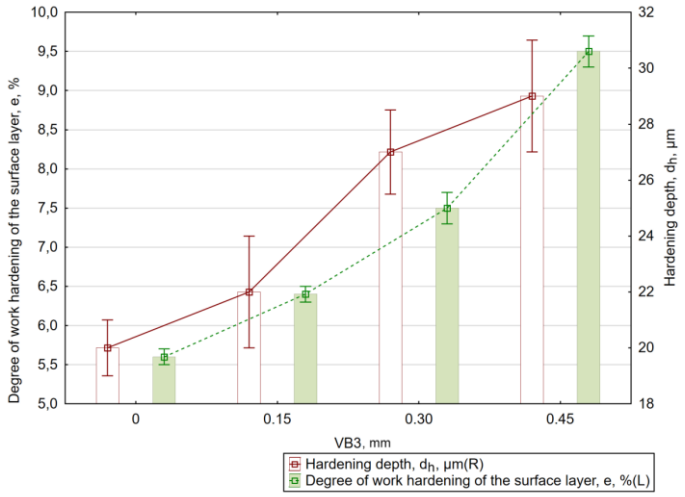

Figure 11. Effect of milling cutter flank wear VB3 on the degree of work hardening of the surface layer and hardening depth.

With increasing the VB_3 wear indicator, a successive increase in the microhardness of the surface layer is observed, expressed both by the degree of work hardening and the hardening depth. After machining with a milling cutter whose cutting edges were characterized by a wear indicator of VB_3 = 0.45 mm, the degree of work hardening increased by approximately 70%, while the hardening depth increased by approximately 45% relative to the values of these parameters after machining with a sharp cutter. The observed microhardness increase should be attributed to the intensified plastic deformation of the subsurface material caused by the greater mechanical load exerted by the worn cutting edge due to the enlarged contact area between the flank face and the workpiece, which results in strain hardening of the surface layer. The obtained results show certain similarities to the findings reported by the authors of [56], who investigated the microhardness of the surface layer of Ti-10V-2Fe-3Al titanium alloy after milling. In [56], the hardening depth was less than 55 µm at VB = 0.2 mm and reached 130 µm at VB = 0.35 mm, which is considerably greater than the values of 20–29 µm obtained in the present study, which may be related to the different properties of the workpiece material and different cutting conditions.

Another investigated property of the surface layer was residual stress. Figure 12 presents a representative distribution of residual stresses in the surface layer of an S2-type specimen that was milled using a tool with its cutting edges characterized by a wear value of VB_3 = 0.45 mm.

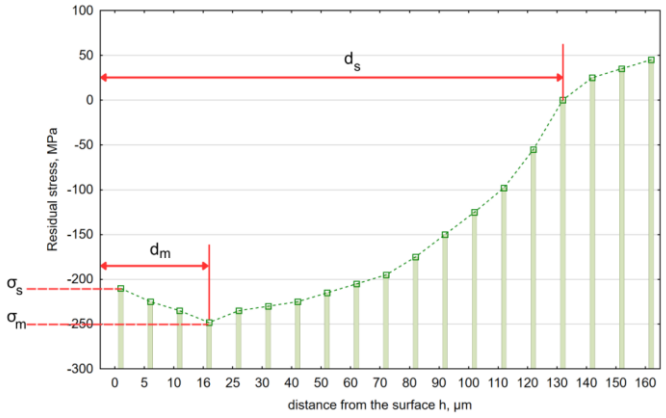

Figure 12. Distribution of residual stresses in the surface layer of the specimen after machining by a milling cutter with a flank wear value of VB_3 = 0.45 mm.

The causes of residual stress formation in the surface layer of a workpiece during milling include both mechanical factors, which are associated with non-uniform plastic deformation, and thermal factors, which are associated with non-uniform material expansion due to heating and cooling. The conducted research indicates that the residual stresses induced in the analyzed titanium alloy milling process are compressive stresses, and therefore their primary cause is of mechanical origin. The compressive residual stresses are generated primarily by the

mechanical effect of the worn flank face pressing against the machined surface, causing plastic deformation of the subsurface material. Upon unloading, the elastically strained surrounding material constrains the plastically deformed zone, resulting in compressive stresses. This effect intensifies with progressive tool wear due to the increasing contact area between the flank face and the workpiece. The following quantities were adopted to characterize the shape of the residual stress distribution curves:

- σ_m – residual stress with the maximum absolute value,
- σ_s – residual stress on the workpiece surface,
- d_m – distance of the stress σ_m from the workpiece surface,
- d_s – depth of occurrence of the compressive residual stresses.

In the surface layer of the specimens milled with worn tools, one can observe higher maximum absolute compressive residual stresses, as well as a greater depth of their occurrence. Similarly to the case of microhardness, this increase should be attributed, to greater plastic deformation of the material during milling conducted with worn cutting edges compared to sharp ones.

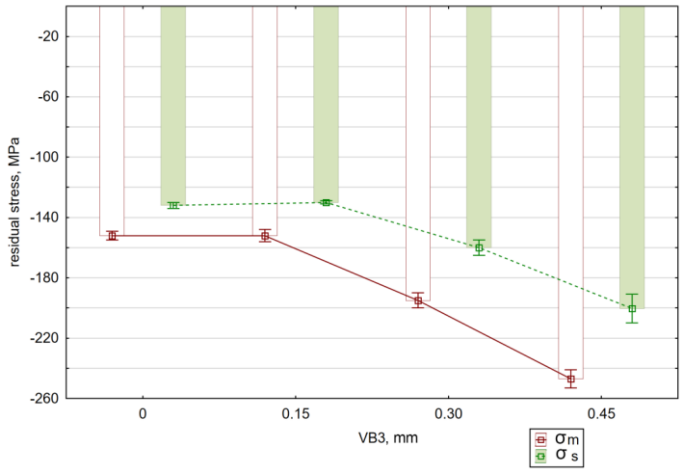

Figure 13. Effect of flank wear VB_3 on the maximum compressive residual stresses in terms of absolute value and the value of residual stresses on the workpiece surface.

The maximum absolute value of compressive residual stresses in the specimens machined using milling cutters with a flank wear value of VB_3 = 0.45 mm was approximately 60% higher compared to that in the specimens machined with sharp milling cutters. A smaller increase in the compressive residual stresses was observed on the specimen surface, amounting to approximately 32% (Fig. 13).

Tool wear causes a significantly greater increase in the depth of residual stress occurrence compared to the increase in the stress values (Fig. 14). After milling using a tool with a flank wear value of VB_3 = 0.45 mm, the compressive residual stresses occurred at a depth approximately 3.2 times greater than after milling with sharp tools. Also, the distance from the surface to the location of the maximum compressive stresses increased by approximately 4 times. Comparing Fig. 11 and Fig. 14, it can be observed that the depth of compressive residual stresses is several times greater than the hardening depth of the surface layer.

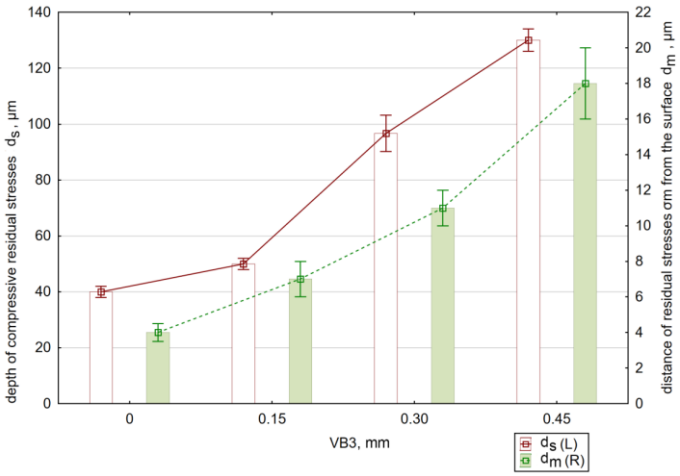

Figure 14. Effect of flank wear VB3 on the depth of compressive residual stresses and the depth of maximum compressive residual stresses below the surface.

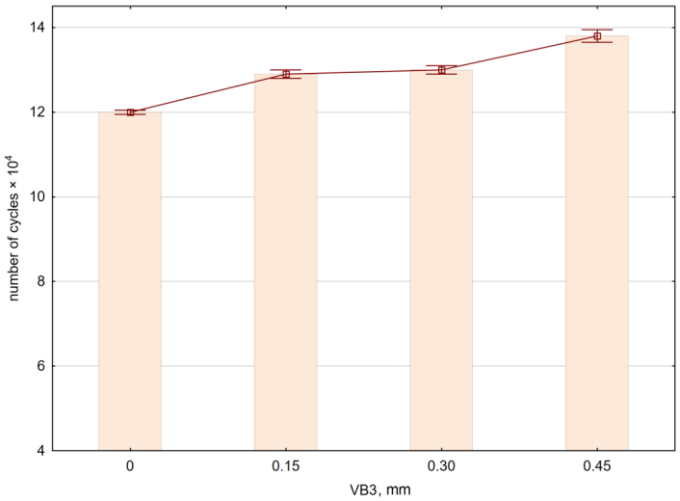

Figure 15. Fatigue life of Ti6Al4V alloy specimens as a function of milling cutter flank wear.

Research on the surface layer properties of machine components is conducted primarily in terms of the functional characteristics of these components. Numerous components

made of Ti6Al4V titanium alloy are subjected to cyclic loading during service, including aerospace components that affect flight safety. The effect of milling cutter flank wear on the fatigue life of machined S3-type specimens, expressed as the number of bending cycles to specimen fracture, is presented in Fig. 15.

A slight increase in the fatigue life of specimens is observed with progressive blunting of the tool cutting edges used for their milling. The fatigue life of the specimens machined with the most worn milling cutters (VB_3 = 0.45 mm) is approximately 16% greater compared to that of the specimens machined with sharp milling cutters. The research results presented above indicate that increasing tool wear leads to an increase both in surface roughness (Fig. 6), which is a factor reducing fatigue life, and in compressive residual stresses (Fig. 13), which, in turn, contributes to an increase in the fatigue life of the machined specimens. Therefore, the conducted research indicates that, for this case, residual stresses have a greater influence on fatigue life than surface roughness. The improvement in fatigue life observed with increasing tool wear can be attributed to the deeper and more intense compressive residual stress fields induced in the surface layer. Compressive residual stresses act by partially offsetting the tensile stresses generated during cyclic bending loading, thereby raising the effective stress threshold required to initiate and propagate fatigue cracks. Furthermore, the increased depth of the compressive stress zone, rising from 40 µm to 128 µm with progressive flank wear, provides a wider subsurface barrier against crack propagation, which is particularly relevant given that fatigue cracks in Ti6Al4V typically initiate at or just below the machined surface.

4. Conclusion

The conducted experimental research was aimed at evaluating the effect of milling cutter flank wear on the surface layer properties of Ti6Al4V titanium alloy specimens. The surface topography, 3D surface roughness parameters, residual stress distribution, and microhardness distribution of the surface layer were investigated. The research was extended to include an assessment of the effect of tool wear on the fatigue life of the milled specimens. Based on the obtained results, the following conclusions were drawn:

- As the milling cutter flank's wear progresses, the texture of the machined surface becomes increasingly irregular; one can observe a lack of continuity of surface asperity peaks and a random distribution of surface valleys.
- The surface roughness obtained after milling can be considered satisfactory for many components manufactured from the titanium alloy under analysis. With increasing tool wear, a slight increase in the surface roughness was observed, from Sa = 0.75 µm at VB_3 = 0 to Sa = 0.90 µm at VB_3 = 0.45 mm.
- Progressive flank wear leads to a substantial increase in thrust force, from approximately 250 N for a sharp tool to 670 N at VB_3 = 0.45 mm, accompanied by a corresponding increase in thrust force amplitude. The increased mechanical load exerted by the worn tool on the machined surface is consistent with the observed enhancement of compressive residual stresses and surface layer hardening.
- During the milling process, compressive residual stresses were induced in the surface layer of the investigated specimens and the microhardness of this layer increased. As the tool wear increased, the maximum compressive residual stresses increased their absolute value from −152 MPa to −245 MPa and their depth of occurrence rose from 40 µm to 128 µm, whereas the degree of work hardening of the surface layer increased from 5.5% to 8.6% and the hardening depth increased from 20 µm to 29 µm.
- The changes in surface layer properties caused by milling cutter flank wear had a beneficial effect on the fatigue life of the investigated specimens, which increased by approximately 16%.

In summary, it can be stated that an increase in the VB_3 flank wear indicator of the cutting edges of cemented carbide inserts mounted in the milling cutter used for Ti6Al4V titanium alloy milling does not cause deterioration in the surface layer condition of the machined specimens; rather, it contributes to a slight increase in their fatigue life. Therefore, milling performed with the technological conditions described in this paper can be used as a finishing operation for titanium alloy components. Based on the obtained results, it is recommended that the flank wear indicator be maintained within $VB_3 \leq 0.45$

mm, as beyond this limit further deterioration of surface roughness may offset the beneficial effect of compressive residual stresses. During the finishing operation, surface roughness (Sa) and, where possible, the distribution of residual stresses in the surface layer should be monitored as key indicators of component functional quality.

References

1. Grochalski K, Jabłoński P, Talar R, Twardowski P, Wieczorowski M, Jakubek B, Rukat W. Temperature Measurement of Modern Cutting Tools During Turning. *Advances in Science and Technology Research Journal* 2020; 14(4): 37-48. https://doi.org/10.12913/22998624/123007.
2. Shan C, Zhang X, Shen B, Zhang D. An improved analytical model of cutting temperature in orthogonal cutting of Ti6Al4V. *Chinese Journal of Aeronautics* 2019; 32(3): 759-69. https://doi.org/10.1016/j.cja.2018.12.001.
3. Bandapalli C, Sutaria BM, Prasad Bhatt DV, Singh KK. Tool Wear Analysis of Micro End Mills - Uncoated and PVD Coated TiAlN & AlTiN in High Speed Micro Milling of Titanium Alloy - Ti-0.3Mo-0.8Ni. *Procedia CIRP* 2018; 77: 626-9. https://doi.org/10.1016/j.procir.2018.08.191.
4. Ciecieląg K. Analysis of the Surface Layer and Feed Force after Milling Polymer Composites with Coated and Uncoated Tools. *Advances in Science and Technology Research Journal* 2023; 17(4): 70-8. https://doi.org/10.12913/22998624/168832.
5. Gerhard N, Brans K, Meurer M, Schraknepper D, Bergs T. Experimental investigation of the friction behavior under cutting conditions. *Procedia CIRP* 2023; 118: 437-42. https://doi.org/10.1016/j.procir.2023.06.075.
6. Zawada-Michałowska M, Pieśko P, Józwik J. Tribological Aspects of Cutting Tool Wear during the Turning of Stainless Steels. *Materials* 2019; 13(1): 123. https://doi.org/10.3390/ma13010123.
7. Twardowski P, Legutko S, Krolczyk GM, Hloch S. Investigation of wear and tool life of coated carbide and cubic boron nitride cutting tools in high speed milling. *Advances in Mechanical Engineering* 2015; 7(6). https://doi.org/10.1177/1687814015590216.
8. Qiu J, Zhang S, Li B, Li Y, Wang L. Research on Tool Wear and Surface Integrity of CFRPs with Mild Milling Parameters. *Coatings* 2023; 13(1): 207. https://doi.org/10.3390/coatings13010207.
9. Zhuang K, Zou L, Weng J, Hu C. Occurrence of catastrophic tool wear patterns through systematic thermomechanical modeling. *Journal of Manufacturing Processes* 2024; 109: 288-99. https://doi.org/10.1016/j.jmapro.2023.12.021.
10. Kumar Wagri N, Petare A, Agrawal A, Rai R, Malviya R, Dohare S, Kishore K. An overview of the machinability of alloy steel. Materials Today: *Proceedings* 2022; 62: 3771-81. https://doi.org/10.1016/j.matpr.2022.04.457.
11. Zhao Z, To S, Wang J, Zhang G, Weng Z. A review of micro/nanostructure effects on the machining of metallic materials. *Materials & Design* 2022; 224: 111315. https://doi.org/10.1016/j.matdes.2022.111315.
12. Klocke F, Krämer A, Sangermann H, Lung D. Thermo-Mechanical Tool Load during High Performance Cutting of Hard-to-Cut Materials. *Procedia CIRP* 2012; 1: 295-300. https://doi.org/10.1016/j.procir.2012.04.053.
13. Abdel-Aal HA, Nouari M, El Mansori M. Influence of thermal conductivity on wear when machining titanium alloys. *Tribology International* 2009; 42(2): 359-72. https://doi.org/10.1016/j.triboint.2008.07.005.
14. Alabort E, Tang YT, Barba D, Reed RC. Alloys-by-design: A low-modulus titanium alloy for additively manufactured biomedical implants. *Acta Materialia* 2022; 229: 117749. https://doi.org/10.1016/j.actamat.2022.117749.
15. Li R, Shih AJ. Tool Temperature in Titanium Drilling. *Journal of Manufacturing Science and Engineering* 2007; 129(4): 740-9. https://doi.org/10.1115/1.2738120.
16. Arrazola PJ, Garay A, Iriarte LM, Armendia M, Marya S, Le Maître F. Machinability of titanium alloys (Ti6Al4V and Ti555.3). *Journal of Materials Processing Technology* 2009; 209(5): 2223-30. https://doi.org/10.1016/j.jmatprotec.2008.06.020.
17. Su H, Liu P, Fu Y, Xu J. Tool Life and Surface Integrity in High-speed Milling of Titanium Alloy TA15 with PCD/PCBN Tools. *Chinese Journal of Aeronautics* 2012; 25(5): 784-90. https://doi.org/10.1016/S1000-9361(11)60445-7.
18. Kuczmaszewski J, Zaleski K, Matuszak J, Pałka T, Mądry J. Studies on the effect of mill microstructure upon tool life during slot milling of Ti6Al4V alloy parts. *Eksploatacja i Niezawodnosc – Maintenance and Reliability* 2017; 19(4): 590-6. https://doi.org/10.17531/ein.2017.4.13.
19. Lebaal N, Nouari M, Ginting A. A new optimization approach based on Kriging interpolation and sequential quadratic programming

algorithm for end milling refractory titanium alloys. *Applied Soft Computing* 2011; 11(8): 5110-9. https://doi.org/10.1016/j.asoc.2011.05.048.

20. Liu E, Wang R, Zhang Y, An W. Tool wear analysis of cutting Ti-5553 with uncoated carbide tool under liquid nitrogen cooling condition using tool wear maps. *Journal of Manufacturing Processes* 2021; 68: 877-87. https://doi.org/10.1016/j.jmapro.2021.06.016.
21. Gupta MK, Niesłony P, Sarikaya M, Korkmaz ME, Kuntoğlu M, Królczyk GM, Jamil M. Tool wear patterns and their promoting mechanisms in hybrid cooling assisted machining of titanium Ti-3Al-2.5V/grade 9 alloy. *Tribology International* 2022; 174: 107773. https://doi.org/10.1016/j.triboint.2022.107773.
22. Gaddam R, Pittala GM, Yussefian NZ, Jamal M, See TL. Study of new solid end mill for side milling of Ti-6Al-4V with improved cooling efficiency. *Procedia CIRP* 2021; 101: 282-5. https://doi.org/10.1016/j.procir.2021.02.031.
23. Da Silva RB, Machado ÁR, Ezugwu EO, Bonney J, Sales WF. Tool life and wear mechanisms in high speed machining of Ti–6Al–4V alloy with PCD tools under various coolant pressures. *Journal of Materials Processing Technology* 2013; 213(8): 1459-64. https://doi.org/10.1016/j.jmatprotec.2013.03.008.
24. Sultana MN, Dhar NR. Performance evaluation of high-pressure cooling by using external rotary liquid applicator in milling Ti–6Al–4V alloy. *Heliyon* 2023; 9(7): e17671. https://doi.org/10.1016/j.heliyon.2023.e17671.
25. Li M, Yue C, Liu X, Zang W, Jiang Z. Diffusion between Ti6Al4V and Cemented Carbide with Different Compositions. *Metals* 2023; 13(2): 240. https://doi.org/10.3390/met13020240.
26. Nouari M, Ginting A. Wear characteristics and performance of multi-layer CVD-coated alloyed carbide tool in dry end milling of titanium alloy. *Surface and Coatings Technology* 2006; 200(18-19): 5663-76. https://doi.org/10.1016/j.surfcoat.2005.07.063.
27. Kim G, Yang SM, Kim DM, Kim S, Choi JG, Ku M, Lim S, Park H. Bayesian-based uncertainty-aware tool-wear prediction model in end-milling process of titanium alloy. *Applied Soft Computing* 2023; 148: 110922. https://doi.org/10.1016/j.asoc.2023.110922.
28. Zanger F, Schulze V. Investigations on Mechanisms of Tool Wear in Machining of Ti-6Al-4V Using FEM Simulation. *Procedia CIRP* 2013; 8: 158-63. https://doi.org/10.1016/j.procir.2013.06.082.
29. Lindvall R, Lenrick F, Persson H, M'Saoubi R, Ståhl JE, Bushlya V. Performance and wear mechanisms of PCD and pcBN cutting tools during machining titanium alloy Ti6Al4V. *Wear* 2020; 454-455: 203329. https://doi.org/10.1016/j.wear.2020.203329.
30. Zareena AR, Veldhuis SC. Tool wear mechanisms and tool life enhancement in ultra-precision machining of titanium. *Journal of Materials Processing Technology* 2012; 212(3): 560-70. https://doi.org/10.1016/j.jmatprotec.2011.10.014.
31. Wang Y, Zou B, Huang C. Tool wear mechanisms and micro-channels quality in micro-machining of Ti-6Al-4V alloy using the Ti(C7N3)-based cermet micro-mills. *Tribology International* 2019; 134: 60-76. https://doi.org/10.1016/j.triboint.2019.01.030.
32. Tan DW, Guo WM, Wang HJ, Lin HT, Wang CY. Cutting performance and wear mechanism of TiB2-B4C ceramic cutting tools in high speed turning of Ti6Al4V alloy. *Ceramics International* 2018; 44(13): 15495-502. https://doi.org/10.1016/j.ceramint.2018.05.209.
33. Ma J, Luo D, Liao X, Zhang Z, Huang Y, Lu J. Tool wear mechanism and prediction in milling TC18 titanium alloy using deep learning. *Measurement* 2021; 173: 108554. https://doi.org/10.1016/j.measurement.2020.108554.
34. Zhao W, Wang S, Han Z, He N. Cutting Performance Evaluation of End Mills for Titanium Aircraft Components. *Procedia CIRP* 2015; 35: 1-7. https://doi.org/10.1016/j.procir.2015.08.051.
35. Tlhabadira I, Daniyan I, Masu L, Mpofu K. Computer aided modelling and experimental validation for effective milling operation of titanium alloy (Ti6Al4V). *Procedia CIRP* 2020; 91: 113-20. https://doi.org/10.1016/j.procir.2020.03.098.
36. Rudawska A, Reszka M, Warda T, Miturska I, Szabelski J, Stančeková D, Skoczylas A. Milling as a method of surface pre-treatment of steel for adhesive bonding. *Journal of Adhesion Science and Technology* 2016; 30(23): 2619-36. https://doi.org/10.1080/01694243.2016.1191585.
37. Daniyan I, Tlhabadira I, Mpofu K, Adeodu A. Investigating the geometrical effects of cutting tool on the surface roughness of titanium alloy (Ti6Al4V) during milling operation. *Procedia CIRP* 2021; 99: 157-64. https://doi.org/10.1016/j.procir.2021.03.097.
38. Polishetty A, Shunmugavel M, Goldberg M, Littlefair G, Singh RK. Cutting Force and Surface Finish Analysis of Machining Additive Manufactured Titanium Alloy Ti-6Al-4V. *Procedia Manufacturing* 2017; 7: 284-9. https://doi.org/10.1016/j.promfg.2016.12.071.
39. Kishore Kumar MS, Gurudatt B, Reddappa HN, Suresh R. Investigations on the effect of Machining parameters on Machining force and roughness in Micro-Milling of Titanium Gr5 and Gr12 alloys under dry Machining conditions using carbide tool. *Materials Today:*

Proceedings 2021; 47: 2598-602. https://doi.org/10.1016/j.matpr.2021.05.082.

40. Wu X, Chen Z, Ke W, Jiang F, Zhao M, Li L, Shen J, Zhu L. Investigation on surface quality in micro milling of additive manufactured Ti6Al4V titanium alloy. *Journal of Manufacturing Processes* 2023; 101: 446-57. https://doi.org/10.1016/j.jmapro.2023.05.110.
41. Lotfi M, Charkhian A, Akbari J. Surface analysis in rotary ultrasonic-assisted milling of CFRP and titanium. *Journal of Manufacturing Processes* 2022; 84: 174-82. https://doi.org/10.1016/j.jmapro.2022.10.006.
42. Ali MH. Studied validation of finite element modeling for titanium alloy (Ti–6Al–4V) at face milling. *Heliyon* 2023; 9(7): e17670. https://doi.org/10.1016/j.heliyon.2023.e17670.
43. Mersni W, Boujelbene M, Ben Salem S, Singh HP. Machining time and quadratic mean roughness optimization in ball end milling of titanium alloy Ti-6Al-4V – Aeronautic field. *Materials Today: Proceedings* 2020; 26: 2619-24. https://doi.org/10.1016/j.matpr.2020.02.553.
44. Sur G, Motorcu AR, Nohutçu S. Single and multi-objective optimization for cutting force and surface roughness in peripheral milling of Ti6Al4V using fixed and variable helix angle tools. *Journal of Manufacturing Processes* 2022; 80: 529-45. https://doi.org/10.1016/j.jmapro.2022.06.016.
45. Polishetty A, Goldberg M, Littlefair G, Puttaraju M, Patil P, Kalra A. A Preliminary Assessment of Machinability of Titanium Alloy Ti 6AL 4V During thin Wall Machining Using Trochoidal Milling. *Procedia Engineering* 2014; 97: 357-64. https://doi.org/10.1016/j.proeng.2014.12.259.
46. Kuczmaszewski J, Zaleski K, Matuszak J, Mądry J. Testing Geometric Precision and Surface Roughness of Titanium Alloy Thin-Walled Elements Processed with Milling. In: Diering M, Wieczorowski M, Brown CA, editors. Advances in Manufacturing II. Cham: Springer International Publishing; 2019. p. 95-106. https://doi.org/10.1007/978-3-030-18682-1_8.
47. Sun C, Shen X, Wang W. Study on the Milling Stability of Titanium Alloy Thin-walled Parts Considering the Stiffness Characteristics of Tool and Workpiece. *Procedia CIRP* 2016; 56: 580-4. https://doi.org/10.1016/j.procir.2016.10.114.
48. Delport LD, Conradie PJT, Oosthuizen GA. Suitable Clamping Method for Milling of Thin-walled Ti6Al4V Components. *Procedia Manufacturing* 2017; 8: 338-44. https://doi.org/10.1016/j.promfg.2017.02.043.
49. Kurpiel S, Zagórski K, Cieślik J, Skrzypkowski K, Kapayeva S, Torekhanova M. Dimensional Deviations of Horizontal Thin Wall of Titanium Alloy Ti6Al4V Determined by Optical and Contact Methods. *Materials* 2023; 16(23): 7272. https://doi.org/10.3390/ma16237272.
50. Stupnytskyy V, Hrytsay I. Comprehensive analysis of the product's operational properties formation considering machining technology. *Archive of Mechanical Engineering* 2020; 67(2): 149-167. https://doi.org/10.24425/ame.2020.131688.
51. Żebrowski R, Walczak M, Klepka T, Pasierbiewicz K. Effect of the shot peening on surface properties of Ti-6Al-4V alloy produced by means of DMLS technology. *Eksploatacja i Niezawodność – Maintenance and Reliability* 2019; 21(1): 46-53. https://doi.org/10.17531/ein.2019.1.6.
52. Chen C, Feng T, Zhang Y, Ren B, Hao Wang, Zhao X. Improvement of microstructure and mechanical properties of TC4 titanium alloy GTAW based wire arc additive manufacturing by using interpass milling. *Journal of Materials Research and Technology* 2023; 27: 1428-45. https://doi.org/10.1016/j.jmrt.2023.10.006.
53. Shokrani A, Dhokia V, Newman ST. Investigation of the effects of cryogenic machining on surface integrity in CNC end milling of Ti–6Al–4V titanium alloy. *Journal of Manufacturing Processes* 2016; 21: 172-9. https://doi.org/10.1016/j.jmapro.2015.12.002.
54. Khosravi J, Azarhoushang B, Barmouz M, Bösinger R, Zahedi A. High-speed milling of Ti6Al4V under a supercritical CO2 + MQL hybrid cooling system. *Journal of Manufacturing Processes* 2022; 82: 1-14. https://doi.org/10.1016/j.jmapro.2022.07.061.
55. Yang P, Yao C, Xie S, Zhang D, Tang DX. Effect of Tool Orientation on Surface Integrity During Ball End Milling of Titanium Alloy TC17. *Procedia CIRP* 2016; 56: 143-8. https://doi.org/10.1016/j.procir.2016.10.044.
56. Houchuan Y, Zhitong C, ZiTong Z. Influence of cutting speed and tool wear on the surface integrity of the titanium alloy Ti-1023 during milling. *The International Journal of Advanced Manufacturing Technology* 2015; 78(5-8): 1113-26. https://doi.org/10.1007/s00170-014-6593-x.
57. Wimmer M, Woelfle CH, Krempaszky C, Zaeh MF. The influences of process parameters on the thermo-mechanical workpiece load and the sub-surface residual stresses during peripheral milling of Ti-6Al-4V. *Procedia CIRP* 2021; 102: 471-6. https://doi.org/10.1016/j.procir.2021.09.080.

58. Köhler J, Grove T, Maiß O, Denkena B. Residual Stresses in Milled Titanium Parts. *Procedia CIRP* 2012; 2: 79-82. https://doi.org/10.1016/j.procir.2012.05.044.
59. Robles A, Aurrekoetxea M, Plaza S, Llanos I, Zelaieta O. Empirical modeling of residual stress profiles in Ti6Al4V after face-milling. *Procedia CIRP* 2022; 108: 362-6. https://doi.org/10.1016/j.procir.2022.03.059.
60. Childerhouse T, M'Saoubi R, Franca L, Weston N, Crawforth P, Jackson M. The influence of machining induced surface integrity and residual stress on the fatigue performance of Ti-6Al-4V following polycrystalline diamond and coated cemented carbide milling. *International Journal of Fatigue* 2022; 163: 107054. https://doi.org/10.1016/j.ijfatigue.2022.107054.
61. Yang D, Liu Z, Xiao X, Xie F. The Effects of Machining-induced Surface Topography on Fatigue Performance of Titanium Alloy Ti-6Al-4V. *Procedia CIRP* 2018; 71: 27-30. https://doi.org/10.1016/j.procir.2018.05.015.
62. Matuszak J, Zaleski K, Zyśko A. Investigation of the Impact of High-Speed Machining in the Milling Process of Titanium Alloy on Tool Wear, Surface Layer Properties, and Fatigue Life of the Machined Object. *Materials* 2023; 16(15): 5361. https://doi.org/10.3390/ma16155361.